ARMY RESEARCH LABORATORY

Microadaptive Flow Control Applied to a Spinning Projectile

by J. McMichael, A. Lovas, P. Plostins, J. Sahu, G. Brown, and A. Glezer

ARL-TR-3589 **September 2005**

NOTICES

Disclaimers

The findings in this report are not to be construed as an official Department of the Army position unless so designated by other authorized documents.

Citation of manufacturer's or trade names does not constitute an official endorsement or approval of the use thereof.

Destroy this report when it is no longer needed. Do not return it to the originator.

Army Research Laboratory
Aberdeen Proving Ground, MD 21005-5066

ARL-TR-3589 **September 2005**

Microadaptive Flow Control Applied to a Spinning Projectile

J. McMichael and A. Lovas
Georgia Tech Research Institute

P. Plostins, J. Sahu, and G. Brown
Weapons and Materials Research Directorate, ARL

A. Glezer
Georgia Institute of Technology

REPORT DOCUMENTATION PAGE

Form Approved
OMB No. 0704-0188

1. REPORT DATE *(DD-MM-YYYY)*	2. REPORT TYPE	3. DATES COVERED (From - To)
September 2005	Final	October 2003–August 2005

4. TITLE AND SUBTITLE
Microadaptive Flow Control Applied to a Spinning Projectile

5a. CONTRACT NUMBER

5b. GRANT NUMBER

5c. PROGRAM ELEMENT NUMBER

6. AUTHOR(S)
J. McMichael,[*] A. Lovas,[*] P. Plostins, J. Sahu, G. Brown, and A. Glezer[†]

5d. PROJECT NUMBER
622618.AH80

5e. TASK NUMBER

5f. WORK UNIT NUMBER

7. PERFORMING ORGANIZATION NAME(S) AND ADDRESS(ES)
U.S. Army Research Laboratory
ATTN: AMSRD-ARL-WM-BC
Aberdeen Proving Ground, MD 21005-5066

8. PERFORMING ORGANIZATION REPORT NUMBER
ARL-TR-3589

9. SPONSORING/MONITORING AGENCY NAME(S) AND ADDRESS(ES)

10. SPONSOR/MONITOR'S ACRONYM(S)

11. SPONSOR/MONITOR'S REPORT NUMBER(S)

12. DISTRIBUTION/AVAILABILITY STATEMENT
Approved for public release; distribution is unlimited.

13. SUPPLEMENTARY NOTES
[*]Georgia Tech Research Institute, Smyrna, GA 30080
[†]Georgia Institute of Technology, Atlanta, GA 30332

14. ABSTRACT
The focus of this report is to provide a technical and programmatic summary of a Defense Advanced Research Projects Agency effort to explore the feasibility of producing steering forces on a spinning projectile using microadaptive flow control (MAFC). The report discusses the theoretical foundation for the flow control mechanism, the multidisciplinary modeling technology developed, the flight control technology required to enable the MAFC on spinning projectiles, the design of the flight test and validation hardware, and the results of the open-loop flight test. The open-loop tests clearly indicate that MAFC can be used as a spinning projectile divert technology and extended to other subsonic munitions. Phase I of the program will conclude with a closed-loop test of the technology. A Phase II program has started to extend the technology to smaller diameter and higher velocity projectiles. The Phase II program will also investigate microgas generators as the MAFC actuator technology.

15. SUBJECT TERMS
microadaptive flow control, guided munition, guided spin-stabilized projectile

16. SECURITY CLASSIFICATION OF:			17. LIMITATION OF ABSTRACT	18. NUMBER OF PAGES	19a. NAME OF RESPONSIBLE PERSON
a. REPORT	b. ABSTRACT	c. THIS PAGE			Peter Plostins
UNCLASSIFIED	UNCLASSIFIED	UNCLASSIFIED	UL	38	19b. TELEPHONE NUMBER (*Include area code*) 410-278-8878

Standard Form 298 (Rev. 8/98)
Prescribed by ANSI Std. Z39.18

Contents

List of Figures

Acknowledgments

The SCORPION (Self Correcting Projectile for Infantry Operation) team consisted of many engineers, scientists, and technicians who contributed to the overall success of the program. The authors of this report would like to recognize the team and express their sincere appreciation for all their efforts.

Georgia Tech Research Institute: Mike Heiges and Kevin Massey

Georgia Tech: Prof. Anthony Calise, Prof. Mark Allen, Brian English, and Chris Rinehart

U.S. Army Research Laboratory: Dave Lyon, Dave Hepner, Tom Harkins, Tim Brosseau, Donald McClellan, Kenneth Paxton, and Brendan Patton

ArrowTech: Wayne Hathaway

Oregon State University: Prof. Mark Costello

1. Program Overview and Objectives

The Future Force Concept for the U.S. Army clearly outlines a strategy for operational scenarios that feature a combined-arms combat system operating in a multithreat, dynamic engagement environment. Precision, small- to medium-caliber munitions are integral and necessary elements of this strategy. To meet this vision, innovative technologies are needed to provide aerodynamic steering forces for small, spinning projectiles.

With support and direction from the Defense Advanced Research Projects Agency (DARPA), the Georgia Institute of Technology and the U.S. Army Research Laboratory (ARL) have teamed on a program called SCORPION (Self Correcting Projectile for Infantry Operation) to develop and explore the applicability of microadaptive flow control (MAFC) technology for aerodynamic steering of spinning projectiles. More specifically, the program is a joint venture between DARPA, the Georgia Tech Research Institute's (GTRI's) Aerospace, Transportation, and Advanced Systems Laboratory, Georgia Tech's Departments of Mechanical Engineering, Electronic and Computer Engineering, and Aerospace Engineering, and ARL's Weapons and Materials Research Directorate.

The SCORPION program is divided into two successive phases: an initial technology feasibility phase and a follow-on technology demonstration phase. The present report summarizes progress to-date on Phase 1, technology feasibility. The specific objective of Phase 1 is to show that MAFC can be integrated into a 40-mm round, an infantry grenade surrogate, to provide sufficient divert control authority and adequate guidance to statistically place the round within a required distance from the target. The second phase, now underway, has the objective of demonstrating that a new MAFC actuator technology based on very small-scale gas generators can be integrated into smaller, faster projectiles to again provide adequate control authority to enable steering and guidance.

The Phase I goals are as follows:

1. Investigate the nonlinear projectile aerodynamics associated with MAFC.
2. Design and implement a piezoceramic actuator-driven synthetic jet system that includes on-board electronic power conditioning and device drivers.
3. Develop an approach for generating aerodynamic control forces using MAFC, and demonstrate that the required divert authority can be generated on low subsonic velocity projectiles.
4. Develop a flight control system for a spin-stabilized infantry grenade with MAFC actuators.

5. Design and build the required miniature high-g sensor and flight control systems.
6. Integrate the actuator and flight control system in a 40-mm projectile test bed.
7. Develop the multidisciplinary tools to model all aspects of the system.
8. Validate all the subsystems with laboratory and flight testing.
9. Perform an open-loop flight test to verify divert authority.
10. Perform and complete a closed-loop system demonstration of the 40-mm system.
11. In parallel with the previous goals, conduct the research necessary to develop alternative actuator concepts for future application to smaller, faster projectiles.

Phase 1 began near the end of FY01 and will be completed in FY04. Goals 1–9 have been completed successfully. Goal 10 will be completed in September 2004. Goal 11 has also been completed, and the concepts and fabrication methods will be further refined and demonstrated during Phase 2. The present report summarizes the work up to and including the accomplishment of goal 9, the open-loop flight test verification of the effectiveness of MAFC-generated steering forces.

The SCOPRION Phase 2 technology demonstration project is a recently launched 30-month follow-on project designed to evaluate advanced microgenerator actuator technology and apply it to achieve adequate MAFC-based divert capability in a high subsonic velocity 25-mm projectile. This will require the development of advanced MAFC approaches and further miniaturization of sensor and flight control systems. This is a critical step towards transitioning MAFC technology into block upgrades to provide guidance for currently planned unguided munition systems such as the 25-mm objective crew served weapon.

The goals of the Phase 2 technology demonstration project are as follows:

1. Develop g-hardened gas generator actuators and fabrication technology.
2. Design, build, integrate, and test power, processor, and driver electronics for gas generator actuator systems.
3. Research the nonlinear aerodynamics associated with the application of MAFC gas-generator actuators to high subsonic velocity spinning projectiles, beginning with 40 mm at lower speeds and continuing to 25-mm projectiles at high subsonic velocities.
4. Integrate actuators and electronics into the flight control system.
5. Miniaturize and g-harden the complete actuator, driver, and flight control system for launch in a surrogate 25-mm projectile.
6. Perform an open-loop divert validation flight test of a gas generator actuator system using a 40-mm projectile at Mach 0.25.

7. Perform an open-loop divert validation flight test of a gas generator actuator system using a 25-mm projectile at Mach 0.6–0.8.

2. Technology Transitioning Strategy

To successfully transition DARPA's advanced MAFC technology rapidly to the warfighter, the product program managers (PMs), e.g., Program Executive Officer of Ammunition, need to have the technology delivered to them in a state that allows a seamless transition to system development and demonstration (SDD). This requires that the following several critical technologies/demonstrations be in place at the end of the program:

1. An integrated set of technology demonstrations of the enabling technology suite.
2. An identified path to the realization of a tactical system, i.e., the ability to integrate other aspects of the system such as the warhead, munition cartridge interface, or safety certifications.
3. An identified path to the required manufacturing capability.
4. A complete modeling and simulation suite of tools to be available for SDD redesign and integration.
5. Early collaboration with the PM so that the technical and financial interface will be in place at the proper transition point.

The current SCORPION program has incorporated specific thrusts in order to address these requirements, including item 5. This philosophy has benefited the program both technically and programmatically by bringing focus, synergy, and overall guidance to the effort. A specific example is the concurrent development of high-performance computing multidisciplinary design tools to model the flow physics and combine the nonlinear fluid dynamics associated with the particular MAFC approach with the nonlinear rigid body flight dynamics. This has helped us understand the complex time-dependent fluid dynamics interaction with the spinning projectile and enabled us to increase the divert forces generated by MAFC. It has also contributed to the definition and design of the flight control system.

The rest of this report will present an overview of past MAFC technologies developed to the present. A discussion of the test article design and subsystem validation will follow as well as the description of the system integration and validation tests. Finally, a short discussion of the planned future work and the transition of the technology to a higher velocity class of projectiles will be presented.

2.1 MAFC Applied to a Spinning Projectile

Synthetic jets were used to develop the control forces on the spinning projectile. Configuration details were derived through a series of tests that used several wind tunnel test models with diameters of 40, 80, and 120 mm. Most of the testing involved the 80-mm model. The final configuration was tested in detail at the 40-mm scale. Synthetic jet actuators were used for the experiments. The wind tunnel model configuration is shown schematically in figure 1.

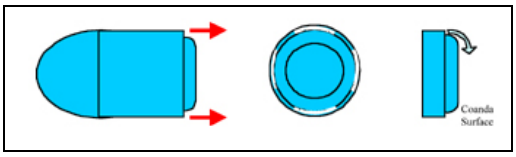

Figure 1. Schematic drawing of 80-mm wind tunnel model configuration.

The general concept is to produce normal (lift) forces by creating an asymmetric flow pattern with separated flow on one side and flow attached to a Coanda surface on the other. Separated flow is created by the rearward-facing step near the aft end of the body, where the lip of the step fixes separation uniformly around the circumference of the body. The wind tunnel model was equipped with four aft-directed synthetic jets located at the base of the backstep; they extended 36°, azimuthally. When one of the jets was activated, it entrained external flow and pulled it around the curved Coanda surface, producing some streamline curvature in the external flow with associated lift on the body.

The effectiveness of this configuration was evaluated experimentally using the wind tunnel apparatus depicted schematically in figure 2.

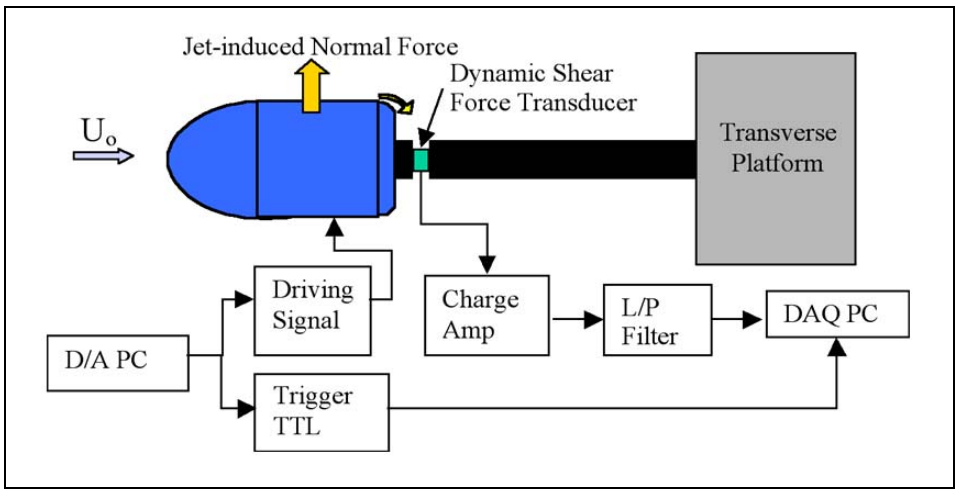

Figure 2. Schematic of wind tunnel test apparatus.

Details of the wind tunnel test results, presented in Rinehart et al. (*1*), are only summarized here. Aerodynamic control forces (and associated moments) are generated using synthetic jet actuators driven by a piezolectric diaphragm operating at its fundamental cavity resonant frequency. This actuation frequency is ~20× higher than the shedding frequency of the body. The flow downstream along the centerline typically turns through nearly 90° at maximum actuator output.

In most of the experiments with the 80-mm model, the radius of the Coanda surface is 13 mm, and the adjoining backward facing step is 1.5 mm high. The step height is shallow enough to enable local flow attachment when the control jet is activated but high enough to prevent attachment in the absence of the jet. The steady lift generated by continuous actuation is shown in figure 3 as a function of jet momentum coefficient.

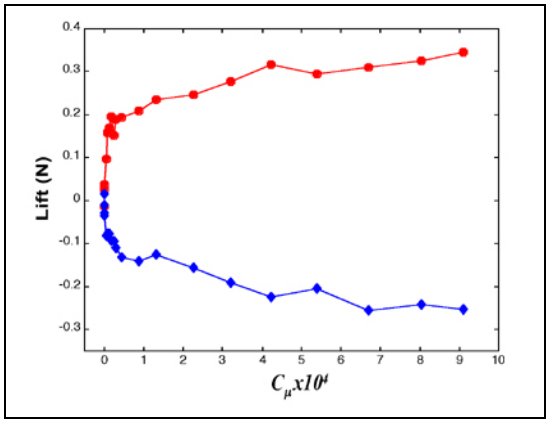

Figure 3. Lift dependence on jet momentum coefficient.

The lift rises dramatically as jet strength increases up to momentum coefficient values of ~5×10^{-5}. This is associated with the initial reattachment of the separated shear layer downstream of the backstep. The lift increases more slowly at higher momentum coefficients as the flow is progressively turned to greater angles around the Coanda surface. Although the jet strength is relatively weak (i.e., the control input is small), with blowing ratios of only ~0.5, the global effect is quite large, with ratios of normal force (lift) coefficient to jet momentum coefficient reaching values as large as 200. This compares to values of this ration of ~80 obtained on two-dimensional airfoils by steady blowing at much higher blowing ratios (*2*).

For a spinning projectile, the control jet cannot be operated continuously. The actuator is in a position to favorably direct a steering force in any given direction for only a portion of a spin cycle, about a quarter cycle, as determined empirically. If the spin period is 16 ms, then only 4 ms are available for the jet to operate, i.e., only four cycles of the synthetic jet diaphragm are available to generate the necessary steering forces. Figure 4 shows the transient force development on an 80-mm body with a free stream velocity of 30 m/s. The jet is operated for 5 ms, about one convective time scale.

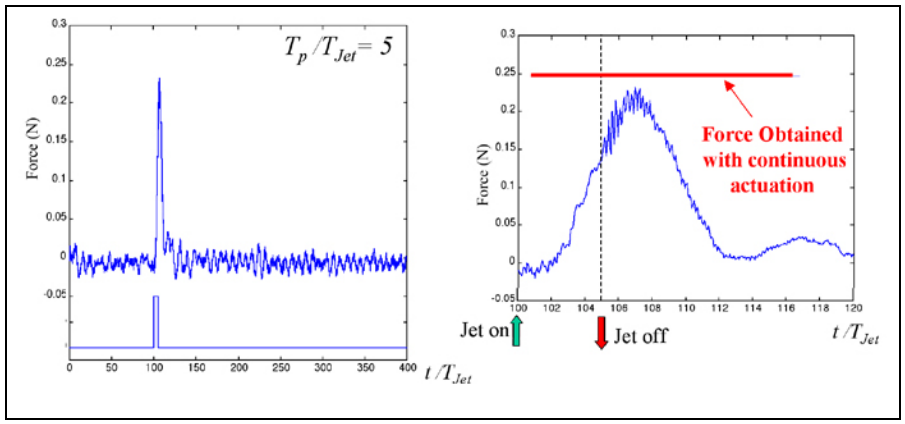

Figure 4. Transient force developed on an 80-mm body at 30 m/s. The jet is operated for 5 ms (about one convective time scale).

To see the flow response to transient activation of the synthetic jet, particle image velocimetry (PIV) measurements were made, phase conditioned to the jet activation signal. The jet was operated for six cycles (6 ms) and then turned off. The flow response is shown in figure 5.

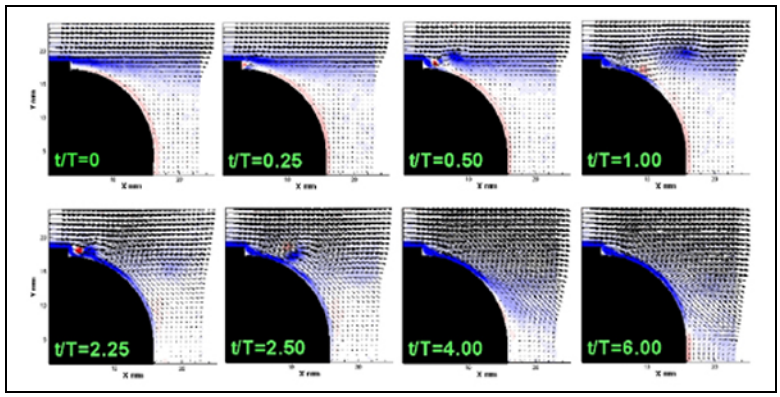

Figure 5. PIV phase-averaged measurements of the flow response to six cycles of synthetic jet activation.

Careful inspection of the figure shows the first vortex pair emerging from the orifice at the first quarter cycle of the jet diaphragm (t/T = 0.25). As this pair grows to full strength, the separated shear layer is cut off, leaving a starting vortex structure in the wake. As the third vortex pair emerges (t/T = 2.25), significant flow turning has already been achieved. Full turning is evident after six diaphragm cycles (about one convective time scale for the 80-mm wind tunnel model).

For a 40-mm spinning body traveling at 70 m/s, the convective time scale is ~1 ms, based on body length (~75 mm). So the flow response should be much faster, and five cycles of jet operation should produce force levels approaching quasisteady values after only 2 or 3 ms. Here, the time scale of the actuator diaphragm is about the same as that for the global flow (convective time scale).

Detailed wind tunnel tests were conducted to examine several aspects of the body and actuator configuration, including Coanda radius and the effect of the step height. An important question concerns the extent to which the flow behaves more or less two dimensionally (axisymmetrically) downstream of the actuator. Near the edges of the jet, the backstep influence can cause significant three-dimensional (3-D) effects. Figure 6 shows the flow turning achieved at the jet centerline, at midspan, and at the edge of the jet.

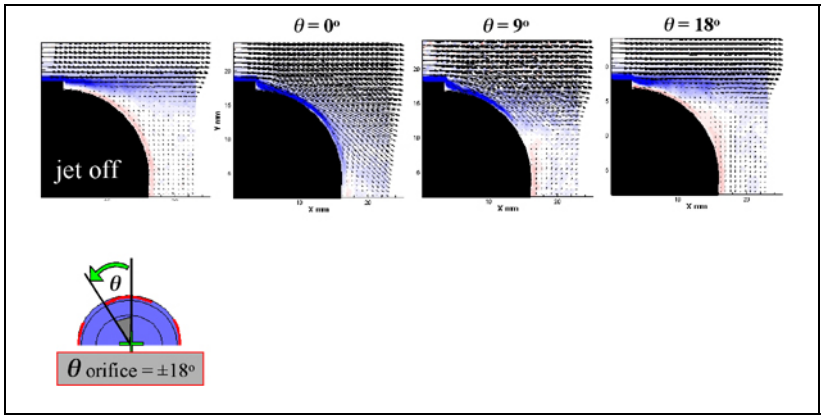

Figure 6. Flow turning as a function of spanwise position with respect to the jet centerline.

It is evident that there is no reattachment at the edge of the (θ = 18°), and that even at midspan the flow detaches after partial turning. It was determined through a series of tests that better attachment could be achieved by reducing the step height and providing a channeled region that, in effect, places strake-like fences at the edges of the channels. The lift force achieved by this modified configuration is shown in comparison to the original configuration in figure 7.

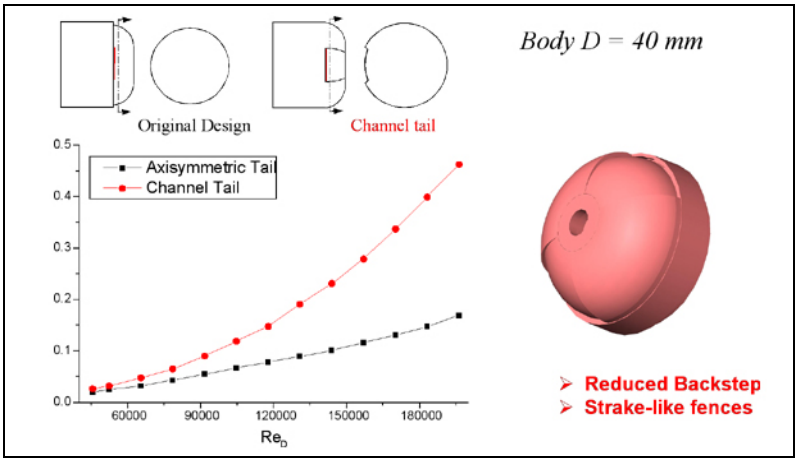

Figure 7. Enhanced force generated by modified aft section configuration.

The net effect is an increase in the force generated under continuous actuator operation by a factor of 2.5, at the higher Reynolds numbers. This is the configuration that was chosen for the flight demonstrations.

Following full system design, g-hardening, and integration, flight tests were conducted to assess the effectiveness of our MAFC approach in generating lateral movement of the projectile in flight. Lateral forces were generated by operating a single synthetic jet actuator at maximum output for one quarter of every revolution. To consistently direct the lateral force, roll angle must be measured. This is because the projectile spin rate decreases along the trajectory, which precludes the use of a simple timing algorithm. On-board magnetometers were used to detect the roll angle and provide an index to the electronic driver for the actuator.

The overall electronic system is shown schematically in figure 8. The on-board system includes batteries, power conditioning, a g-switch to sense launch, magnetometers to measure roll angle, a processor to determine when the actuator is in the proper position to produce a force in the desired direction (left or right), and the driver that provides the oscillatory signal to the synthetic jet diaphragm when the body is at the proper range of roll angles.

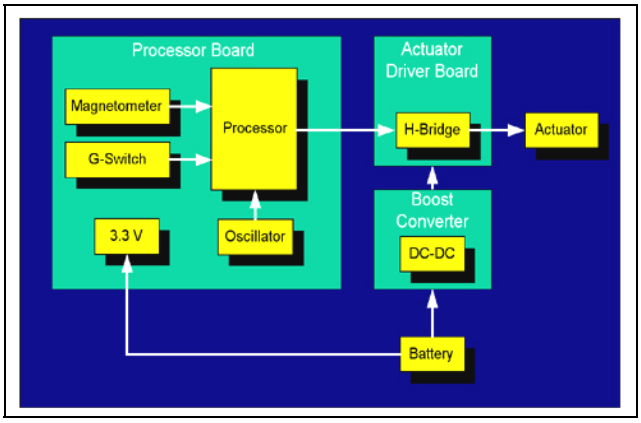

Figure 8. Overall schematic of the electronic control system for the open-loop flight tests.

2.2 Computational Fluid Dynamics (CFD) Modeling

As part of the DARPA SCORPION program advanced state-of-the-art, time-accurate CFD techniques have been developed and applied to a new area of aerodynamic research on synthetic jets for control of subsonic projectiles. Cutting-edge CFD technology has been successfully applied to modeling microadaptive flow control. This research has provided an increased fundamental understanding of the complex, 3-D, time-dependent aerodynamic interactions associated with microjet control for yawing spin-stabilized projectiles. Detailed flow physics simulations have captured all the flow structures with high fidelity and successfully identified the locations of synthetic microjets for optimum aerodynamic interference and control authority.

The control of the trajectory of a 40-mm spinning projectile is achieved by altering the pressure distribution on the projectile through forced asymmetric flow separation (figures 9 and 10) using the Coanda effect (*3*, *4*). Time-accurate CFD modeling capabilities were developed and used to assist in the design of the projectile shape, the placement of the synthetic actuators, and the prediction of the aerodynamic force and moments for these actuator configurations. Additionally, the advanced CFD capabilities provided a simpler way to explore various firing sequences of the actuator elements.

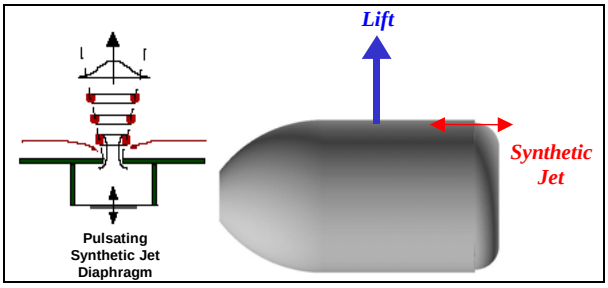

Figure 9. Schematic of synthetic jet and its location on the instantaneous velocity projectile.

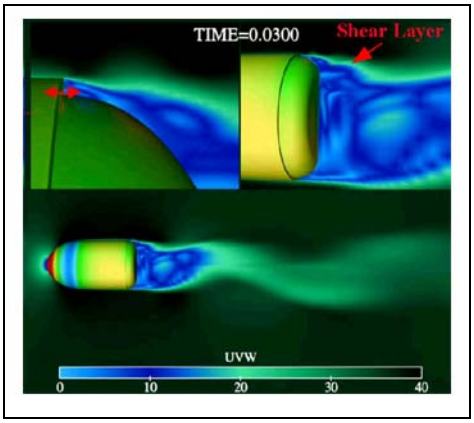

Figure 10. Computed magnitude contours.

Time-accurate unsteady CFD computations were performed to predict and characterize the unsteady nature of the synthetic jet interaction flow field produced on the projectile for various yaw and spin rates for fully viscous turbulent flow conditions. Turbulence was initially modeled using a traditional Reynolds-Averaged Navier-Stokes (RANS) approach. Although this approach provided some detailed flow physics, it was found to be less accurate for this new class of unsteady flows associated with synthetic jets. In order to improve the accuracy of the numerical simulation, the predictive capability was extended to the higher-order hybrid RANS/LES (large eddy simulation) approach (*5*). This new approach computed the large eddies present in the turbulent flow structure and allowed the simulation to capture, with high fidelity,

additional flow structures associated with the synthetic jet interactions in a time-dependent fashion. Modeling of azimuthally-placed synthetic microjets required tremendous grid resolution, highly specialized boundary conditions for the jet activation, and the use of advanced hybrid LES approach permitting local resolution of the unsteady turbulent flow with high fidelity. The addition of yaw and spin while the projectile is subjected to the pulsating microjets rendered predicting the forces and moments as a major challenge.

This capability has provided fundamental understanding of fluid dynamics mechanisms associated with the interaction of the unsteady synthetic jets and the projectile flow fields (*6*). Many flow-field solutions resulting from the simulation of multiple spin cycles, and hence a large number of synthetic jet/flow fields, were saved at regular intermittent time-intervals to produce movies to gain insight into the physical phenomenon resulting from the synthetic jet interactions. The unsteady jets were discovered to break up the shear layer coming over the step in front of the base of the projectile. It is this insight that was found to substantially alter the flow field (making it highly unsteady) both near the jet and in the wake. This, in turn, resulted in asymmetric pressure distributions that produced the required forces and moments even at 0° angle of attack. Time-accurate velocity magnitude contours (figure 2) confirm the unsteady wake flow fields arising from the interaction of the synthetic jet with the incoming free stream flow at Mach = 0.24. Figure 11 shows the particles emanating from the jet and interacting with the wake flow, making it highly unsteady. More importantly, the breakup of the shear layer is clearly evidenced by the particles clustered in regions of flow gradients or vorticity. Verification of this conclusion is provided by the excellent agreement between the predicted (solid line) and measured (solid symbols) values of the net lift force due to the jet (figure 12) for a nonspinning case at GTRI. The net lift force was determined from the actual time histories of the highly unsteady lift force. An example of the time-dependent aerodynamic forces resulting from the jet interaction (jet is on and off during spin cycle) for the actual spinning case at 0° angle of attack and computed with the new hybrid RANS/LES turbulence approach is shown in figure 13. The computed lift force, along with other aerodynamic forces and moments and directly resulting from the pulsating jet, was then used for the design of the actuator, flight control, and sensor system required to provide the desired course correction for the projectile. The results showed the potential of CFD to provide insight into the jet interaction flow fields and provided guidance as to the locations and sizes of the jets to generate the maximum control authority required to maneuver a spinning projectile to its target with precision. In addition, a multidisciplinary coupled CFD and rigid body dynamics technique was developed and demonstrated the effect of microadaptive flow control on the flight trajectories through a “virtual” fly-out of a projectile on the supercomputers.

The ability to use the advanced CFD simulation of this complex flow field was critical to understanding the microadaptive flow control mechanism and a successful open-loop diverting projectile design. This research is at the forefront of technology in the projectile aerodynamics

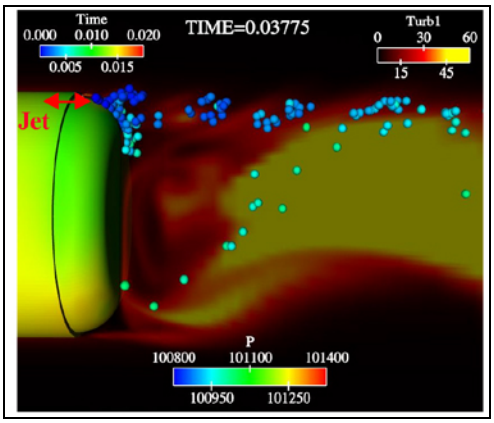

Figure 11. Instantaneous particle traces in the wake.

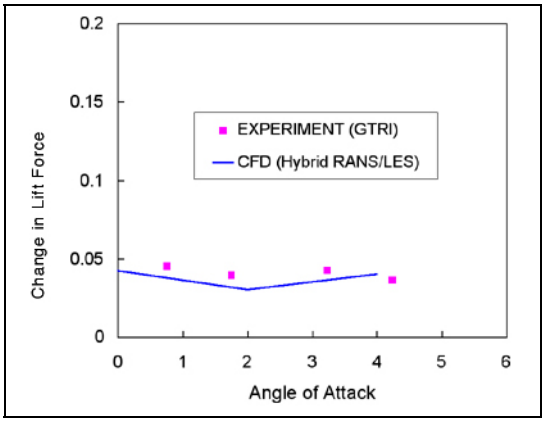

Figure 12. Lift force due to the jet vs. angle of attack.

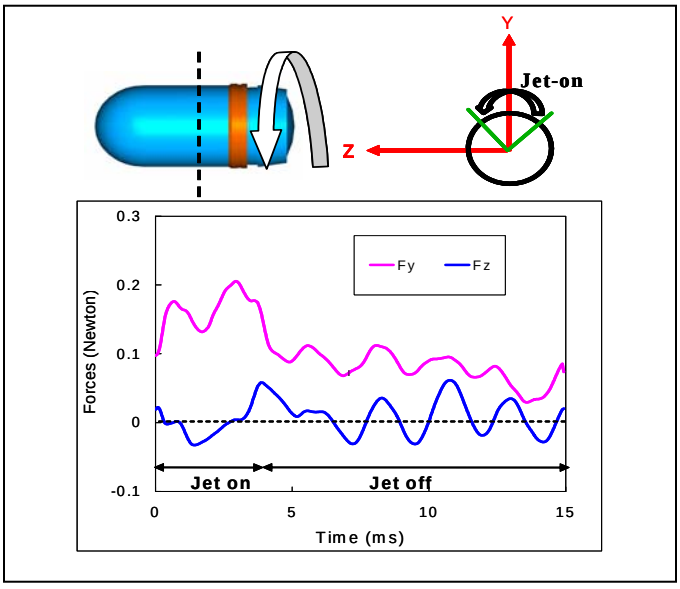

Figure 13. Time-averaged aerodynamic forces.

area and represents a major increase in capability for determining the unsteady aerodynamics of projectiles in a new area of flow control. This research has shown that microadaptive flow control with tiny synthetic jets can provide an affordable route to lethal precision-guided infantry weapons.

2.3 Projectile Design

The testbed projectile for the SCORPION program is based on the M781BT practice grenade. This testbed projectile was chosen because cartridge hardware, propellant, and launch tubes were readily available for the program. In order to determine if the projectile could be diverted, it was first necessary to get a complete aerodynamic characterization of the nonlinear flight dynamics of the base design. It was required to assess the aerodynamics over the entire trajectory as well as develop a ground truth system to evaluate the functionality of all of the subsystems in flight. To this end, a complete telemetry and sensor system was designed for the projectile. The basis for this telemetry and sensor system is the ARL DFUZE described in references (*7–9*). Since the grenade is tube launched at ~10 kg, a comprehensive in-bore model was developed to predict the in-bore launch forces (*10–12*). This modeling effort was combined with specific high-g laboratory testing of the subsystem technologies to verify launch survival. The tactical configuration could not be used because wind tunnel tests of the microadaptive flow control concept using the Coanda effect indicated that a smooth forebody was required to achieve the desired effect. A sabot/pusher system was developed and tested to launch the configuration required. A short summary and selected examples of each of these efforts will be presented in the next sections.

2.4 Aerodynamics

The 40-mm grenades are subsonic projectiles with highly nonlinear aerodynamics. The projectiles are spin stabilized and have classic magnus moment instabilities that result in yaw growth and limit cycles during the downrange trajectories. This was the first attempt to develop a flight control and divert system for a highly spun projectile with this class of nonlinearity. It was therefore important to understand all of the aerodynamic nonlinearities and flight dynamics along the entire trajectory. This data would allow the design of a controller that could divert the round without driving it unstable prior to impact.

A series of aerodynamics tests were conducted in the Aerodynamics Experimental Facility (AEF) (*13*). The AEF is an indoor orthogonal spark shadowgraph test facility designed to obtain complete projectile and missile aerodynamics. It contains 37 orthogonal spark shadowgraph stations over 100 m of instrumented length. It can obtain both linear and nonlinear aerodynamics of flight vehicles from 2 to 40 mm in diameter. The facility can provide both static and dynamic aerodynamic stability derivatives. The SCORPION baseline projectile was tested, and a complete set of nonlinear aerodynamic coefficients was obtained. These coefficients included drag, yaw drag, lift, moment, pitch damping, roll damping, magnus moment, and cubic magnus

moment (*14*, *15*). Figure 14 is a photograph of the AEF, and figure 15 is a spark shadowgraph of the 40-mm projectile in flight at Mach 0.5. The data clearly showed that the projectile had the classic fast mode/slow mode angular behavior (see figure 16). The projectile showed a magnus instability in the fast mode (see figure 17). Over the length of the measurement distance in the AEF, 60 m, a small growth in the fast mode can be noted. This warranted further investigation and was addressed with a long-range free flight using the telemetry system described in the next section. It was necessary to do this to ascertain the exact extend of the yaw growth along the trajectory of interest.

Figure 14. AEF.

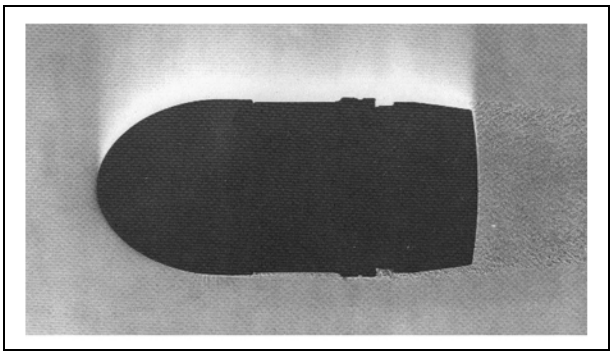

Figure 15. The 40-mm projectile at Mach 0.69.

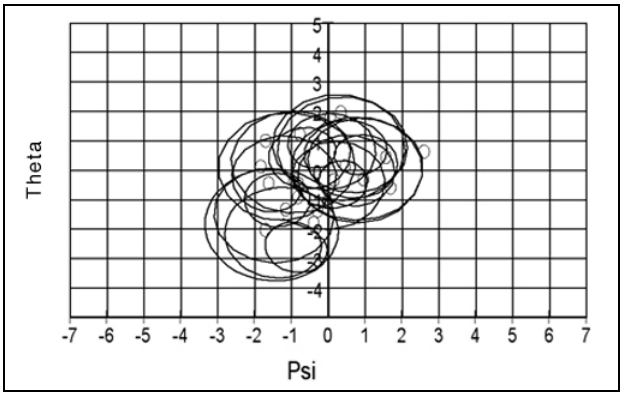

Figure 16. Pitch vs. yaw measured in the AEF.

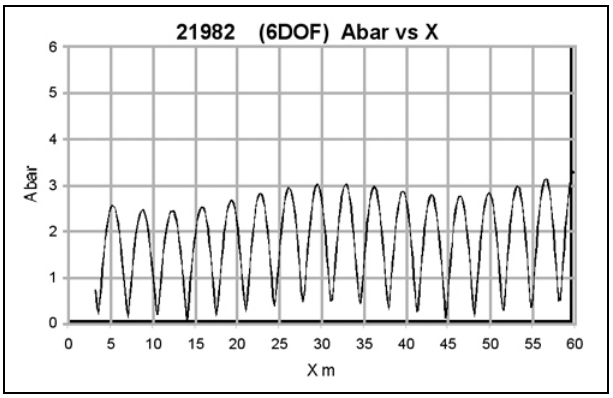

Figure 17. Total yaw vs. range.

2.5 In-bore Launch Modeling and Validation Testing

In order to understand the launch behavior of the projectile, DYNA3D was used to analyze the projectile mechanical behavior and dynamic response. This was necessary in order to design for the survivability of the on-board electronics during the in-bore launch. The forward launch loads are ~ –10 kg; however, significant transverse loads due to balloting can also damage the electronic subsystems. The simulation model consisted of 17 components and five materials (see figure 18). The stress states and deformation in different parts are analyzed as a function of in-bore time. The projectile muzzle exit velocity and the maximum acceleration in-bore were matched to experimental data to ensure simulation fidelity. Two composite boards inside the projectile are studied in detail to ensure that the deformation was small enough so that the electronic components were not effected during the launch. The projectile is launched from a rifled barrel; the full spin rate is modeled in DYNA3D.

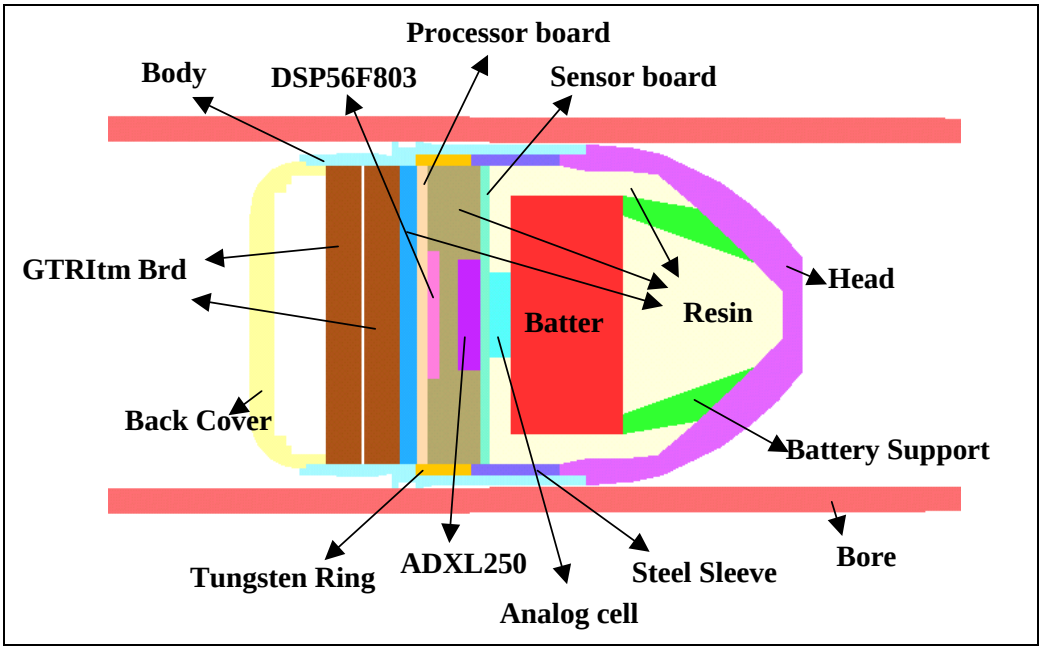

Figure 18. Telemetry system design.

Critical components were also tested for high-g survivability in high-g laboratory facilities of ARL. A specific example of the results will be given for the piezoceramic actuators.

In order to investigate the SCORPION dynamic mechanical response and launch behavior, a finite-element method was used to perform a full-scale simulation. A full 3-D Lawrence Livermore National Laboratory code, DYNA3D (*11*), was adopted for the analysis. The input required includes geometric data, mechanical data, and projectile base pressure. Using the computer-aided design (CAD) software SOLID WORKS (*16*), the SCORPION finite-element analysis (FEA) model was generated. There are a total of 17 modeled parts in the model. The interfaces of each part are guaranteed to be geometrically accurate by using the CAD package. The model input mechanical data includes modulus, poison ration, and density. The mechanical properties for most of the parts are available from the engineering handbook (*17*). For the unavailable mechanical data required for the chips and potting compound, reasonable values are estimated. The projectile base pressure is obtained from the experimental data and matched to interior ballistic calculations. The ARL IBHVG2 interior ballistics code was used to predict the in-bore and projectile base pressure history (*18*). The in-bore acceleration history is given in figure 19 and the velocity in figure 20.

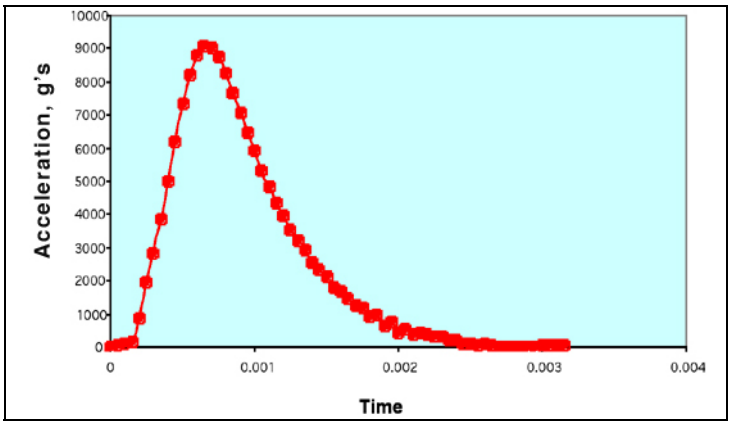

Figure 19. SCORPION in-bore acceleration history.

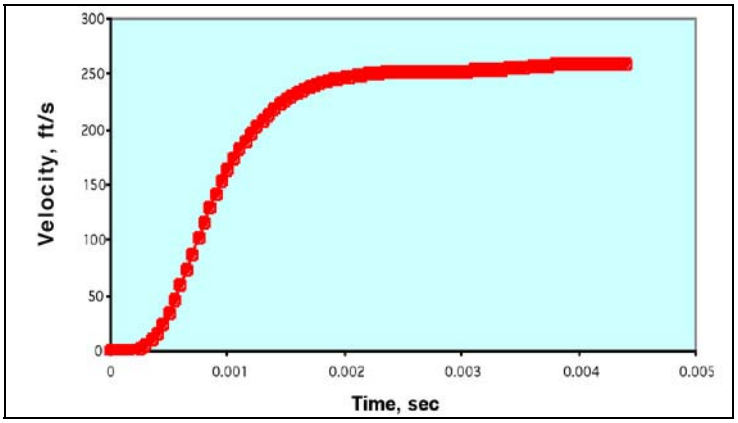

Figure 20. SCORPION in-bore velocity history.

The meshes used on the DYNA 3-D FEA model are shown in figures 21 and 22. The need for the complete dynamic FEA simulation is clearly seen in figure 23. The smooth acceleration load predicted by the IBHVG2 code is not what the projectile experiences; this is the smooth line in figure 23. The simulation clearly shows the high-frequency dynamic state of stress experienced by the projectile. This environment has g-loads that peak at least 2.5× higher than the g-load predicted by IBHVG2. These high-frequency loads are usually responsible for damaging the electronics during gun launch. The simulation indicated that the rear sensor board was subjected to significant stress levels; this is the high stress red area in figure 24. This information was used to help design the mounting and potting system for the electronics boards needed for the telemetry and guidance systems.

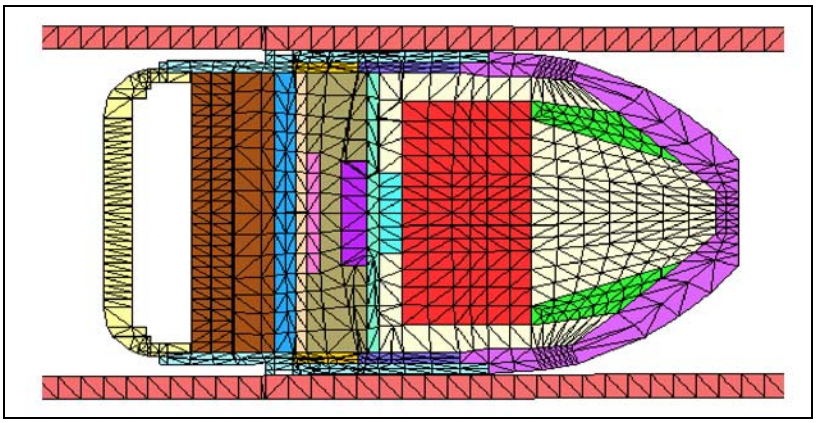

Figure 21. FEA meshes inside the SCORPION projectile with the barrel.

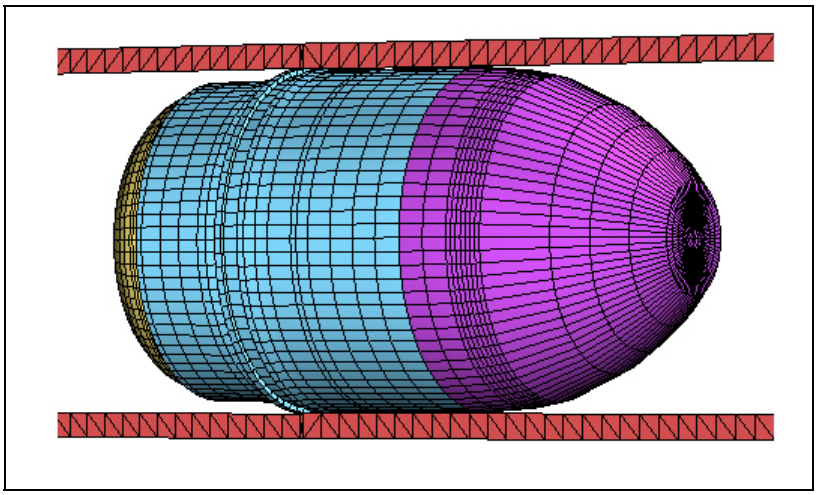

Figure 22. Mesh on the surface of the SCORPION projectile with the barrel.

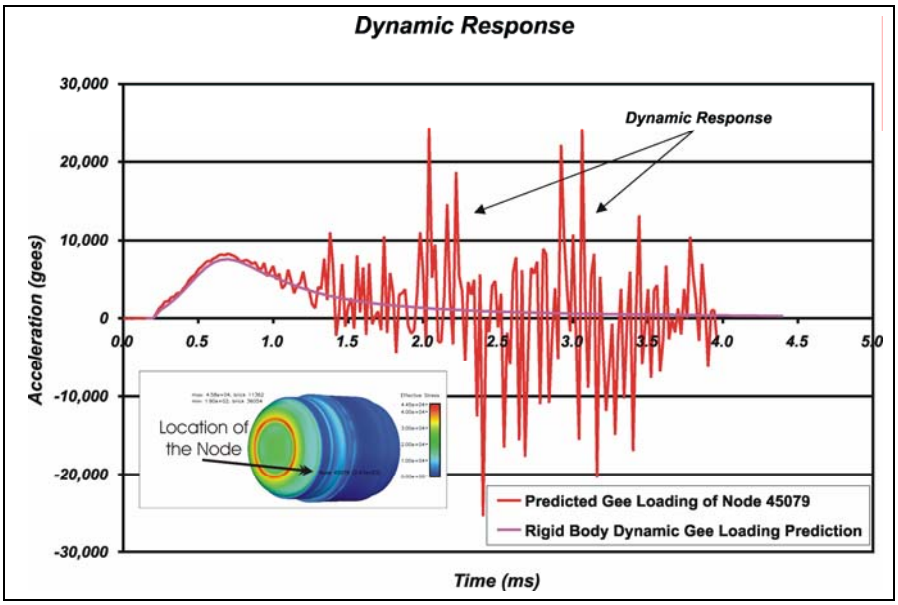

Figure 23. The predicted acceleration load at a given node on the projectile.

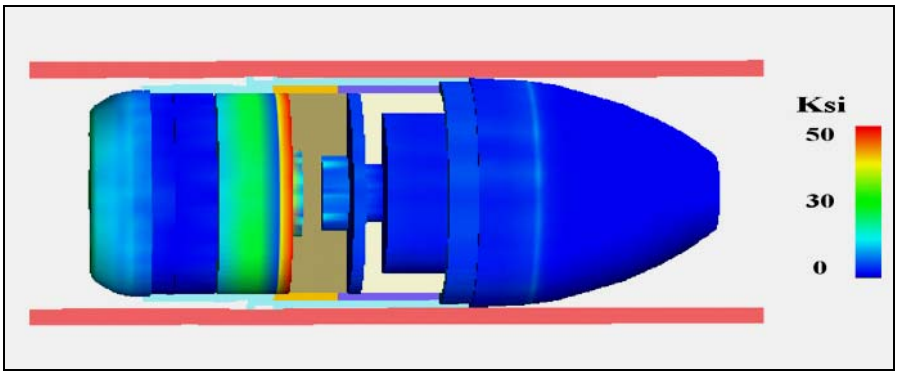

Figure 24. Effective stress contours inside the projectile.

All of the subsystems used in the program were shock tested and then gun launched in surrogate projectiles. If the components passed the shock tests in the laboratory, they were integrated into specially-designed projectile surrogates to verify launch survivability. This was necessary since the effect of spin could not be duplicated in the laboratory tests. These projectiles were recovered after gun launch, and the subsystems were retested for function and compared to the no-load performance. The example given here is for the piezoceramic actuators that are used to divert the projectile. The actuators were shock table tested to 9600 g. An M781BT projectile was modified to carry the actuators out of the gun. The modified projectile with the actuator mounting is shown in figure 25. Two projectiles were launched with maximum g-loads of 6800 and 8538 g, respectively. Figure 26 is a comparison of the variation of maximum jet velocity vs. frequency before and after the gun launch test. Clearly, the piezoceramic actuator survived the gun launch intact and functioning.

Figure 25. M781BT projectile with actuator mounting.

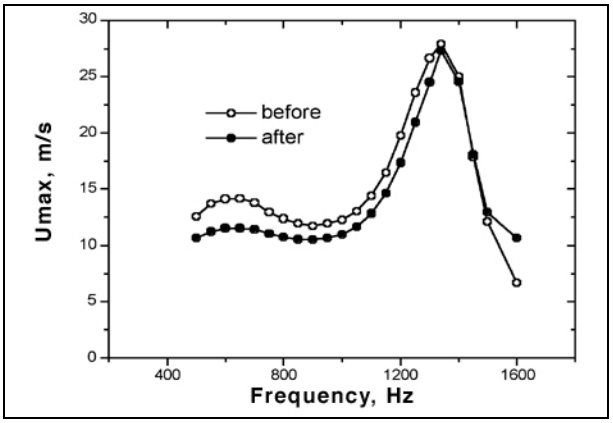

Figure 26. Before and after gun launch validation of actuator jet velocity.

2.6 Telemetry System Design

A telemetry system was designed for the SCORPION projectile and program. The purpose was twofold—(1) to provide a ground truth sensor system for subcomponent tests and (2) to be used as the sensor suite for the guidance navigation and control system. The SCORPION telemetry system is based on the ARL DFUZE sensor system (*7*, *8*). The system has a three-axis magnetometer, four radial accelerometers, an axial accelerometer, and a two-axis accelerometer for transverse acceleration. The system also has a suite of four Yawsondes (*9*). The magnetometers are used to measure the projectile orientation to the earth's magnetic field as well as the roll angle. The Yawsondes measure the projectile angular orientation to the sun. This set of angles completely identifies the angular state of the projectile. The accelerometer suite measures the accelerations in the *x*, *y*, and *z* directions. An encoder board is included to process the data and telemeter the data to the ground station. Figure 27 is a photograph of the front and back side of the DFUZE sensor suite. Figure 28 contains photographs of the SCORPION.

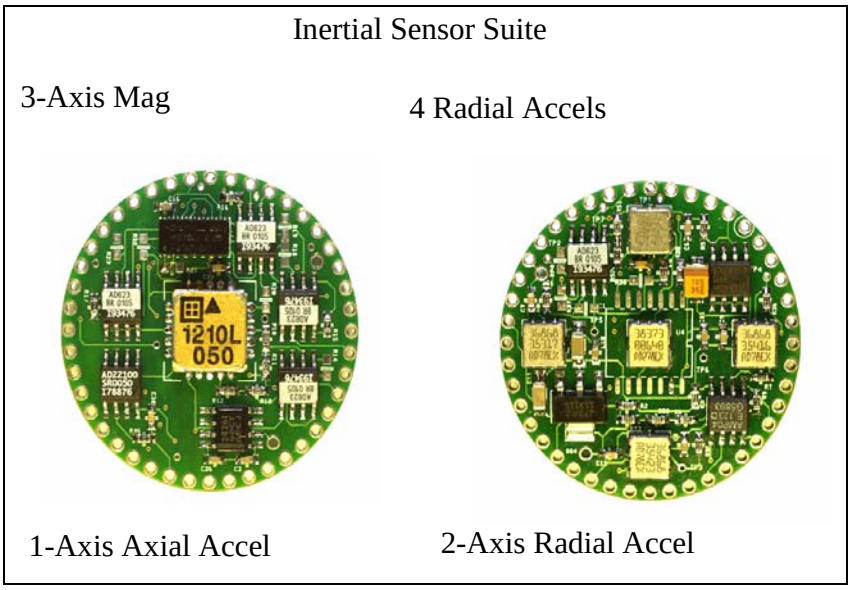

Figure 27. Front and back view of the DFUZE sensor board.

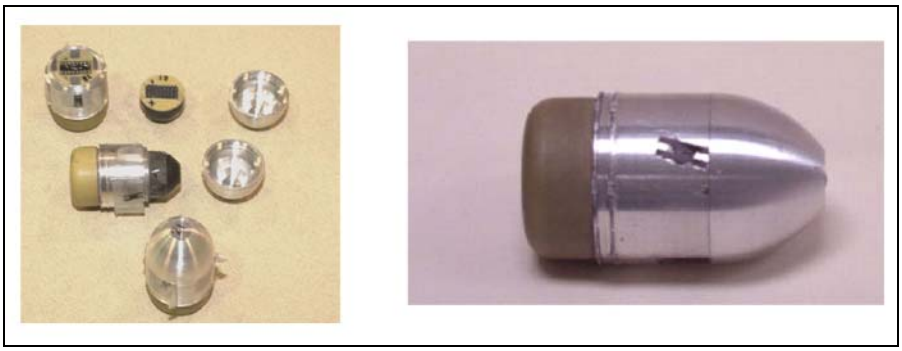

Figure 28. Photographs of the SCORPION telemetry projectile showing the radome and battery and projectile assembly. Telemetry projectile showing the radome for the telemetry antenna and the battery and the projectile assembly showing the Yawsonde slit.

The telemetry system was used to obtain the projectile flight dynamics along the trajectory. Figure 29 is the magnetometer data from a SCORPION flight. The data confirmed that the projectile has a slowly growing fast mode magnus instability. The data was used to update the aerodynamics model and do trajectory modeling that showed that the divert forces derived from the Coanda effect would not overdrive the flight dynamics. The telemetry test was critical in proving that a spin-stabilized projectile with nonlinear aerodynamics could be diverted and controlled.

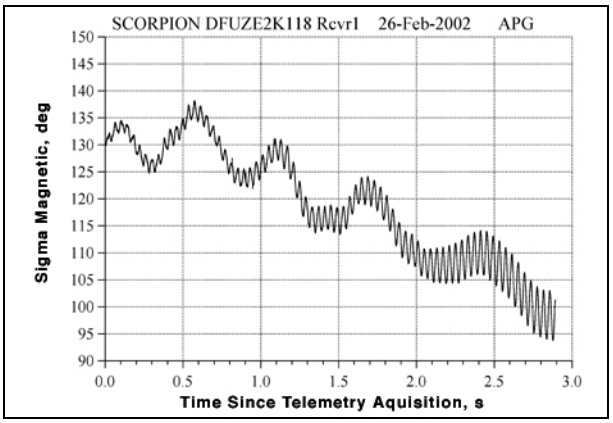

Figure 29. Magnetometer data showing the projectile angle relative to the earth's magnetic field.

2.7 System Integration and Validation Testing

All the previous research, data, wind tunnel testing, computational modeling, and validation were used to design the integrated projectile system for an open-loop test to demonstrate that trajectory divert could be achieved using microadaptive flow control and the Coanda effect. The open-loop test required the design of a launch system, a sensor system, a processor system, an actuator driver board, and the actuator Coanda surface interface. The layout of the projectile is presented in figure 30, and a solid model of the projectile is shown in figure 31. The Coanda surface had to be fitted with fences to enhance the jet interaction. This was determined from wind tunnel tests performed at GTRI. The fences can be seen in the close-up of the projectile base in figure 32. The wind tunnel tests also indicated that the aerodynamic surface of the projectile needed to be smooth as it approached the step where the actuator orifice is located in order for the Coanda effect to develop the divert force. This fact required a sabot pusher system to be developed in order to launch a projectile that did not have an obturator band on the projectile body forward of the step. This pusher sabot was successfully developed and tested in the ARL AEF. A photograph of the sabot pusher is given in figure 33, and figure 34 provides a high-speed launch photograph of sabot pusher separation.

The open-loop test flight control system was designed to initially divert at a given distance from the gun muzzle and then continuously divert to the left or the right. The test was conducted at the ARL Transonic Experimental Facility. Figure 35 is photograph of the test setup looking downrange towards the 200-m target. The sensor system measured its orientation to the earth's magnetic field and thus determined the appropriate divert direction. The projectile flight control system was reprogrammable; this feature was used extensively. The electronic and sensor system proved to be so robust that one projectile was reprogrammed and launched 10 times. It was still functional at the end of the test. The flight control system is shown in figure 36. As with the sensor and telemetry system, the divert flight control system was assembled and g-tested prior to final assembly. The system was potted, g-tested, x-rayed to verify structural

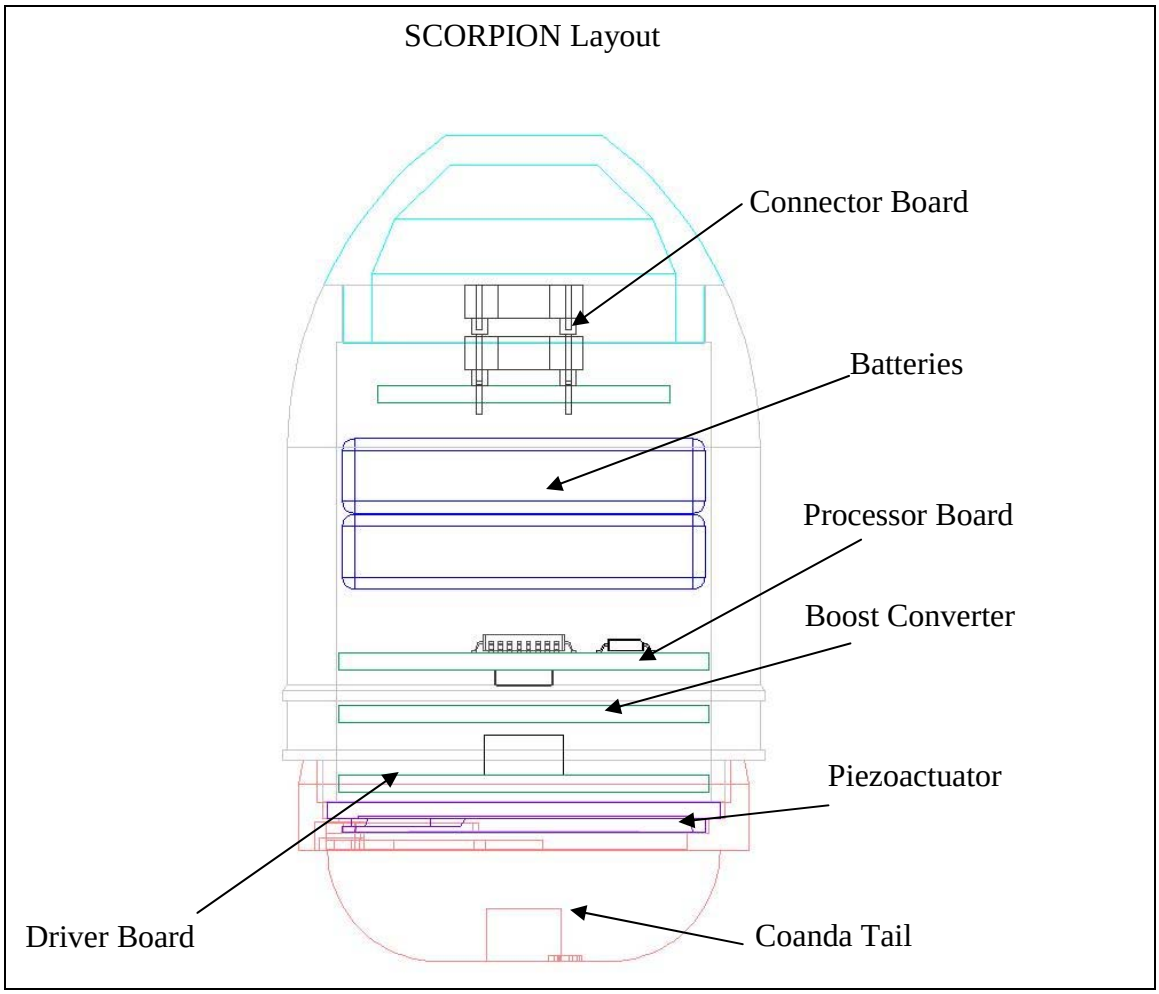

Figure 30. Open-loop test projectile layout.

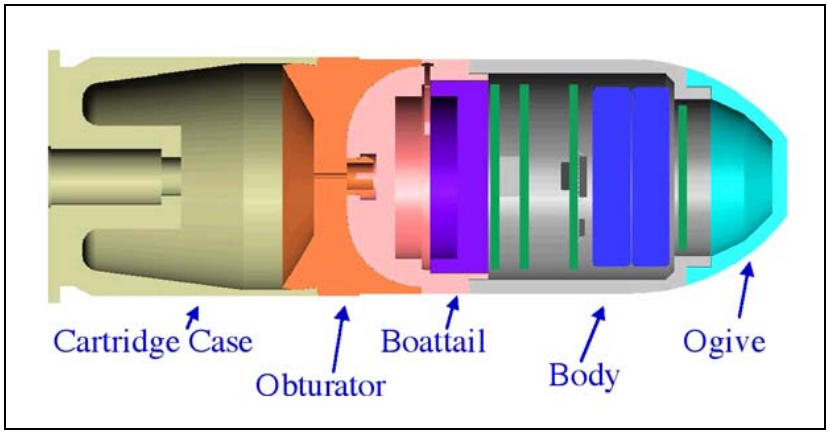

Figure 31. Solid model of open-loop projectile, sabot, and cartridge case.

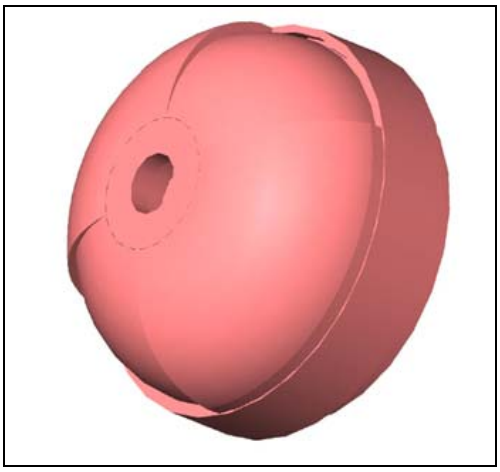

Figure 32. Close-up of SCORPION projectile base showing jet orifice and Coanda surface fences.

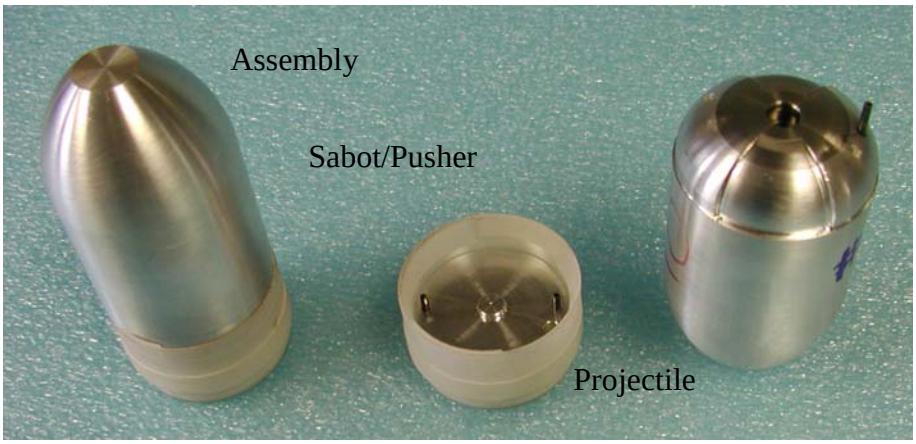

Figure 33. Projectile assembly and sabot pusher system.

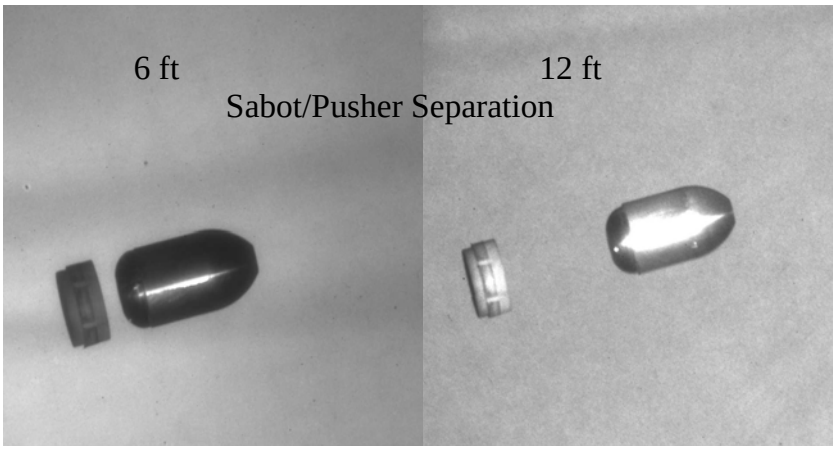

Figure 34. Projectile launch at 82 m/s and sabot pusher separation.

Figure 35. SCORPION open-loop test setup at the ARL Transonic Experimental Facility.

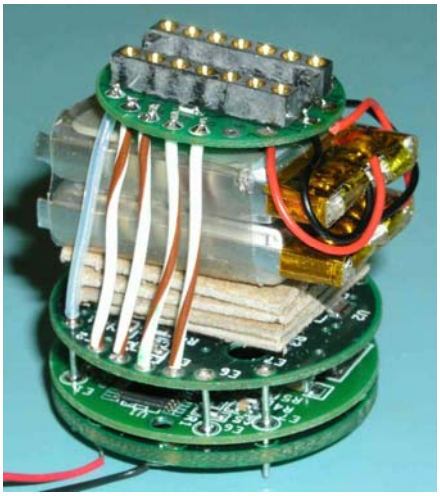

Figure 36. Unpotted SCORPION open-loop flight control and sensor system.

integrity, and then bench tested. Photographs of the unpotted assembly and the pre- and post-g-test x-rays are shown in figure 37. The final assembly and assembly components are given in figure 38.

The open-loop test successfully demonstrated the divert authority of the system. The projectiles were programmed to divert both left and right, and the impacts measured on the target at 200 m. These results can be seen in figure 39. Also plotted in the figure are simulations of the divert simulated data using the BOOM code (*19*). The code is a full 6 degree-of-freedom trajectory simulation including an imbedded model of the guidance navigation and control sensors. The

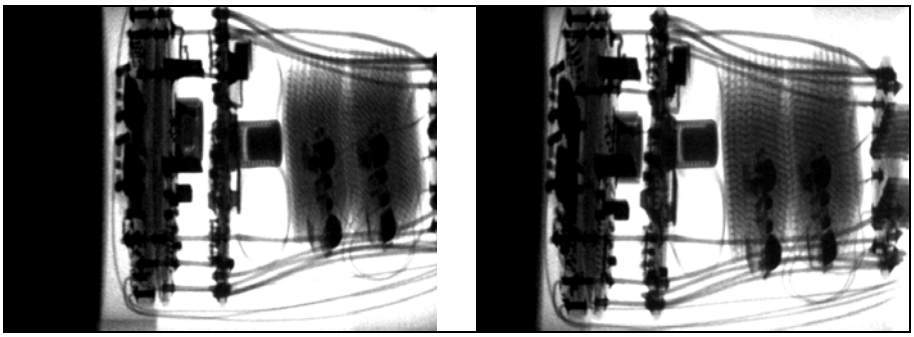

Figure 37. X-rays of potted sensor system before and after 8000 g-test.

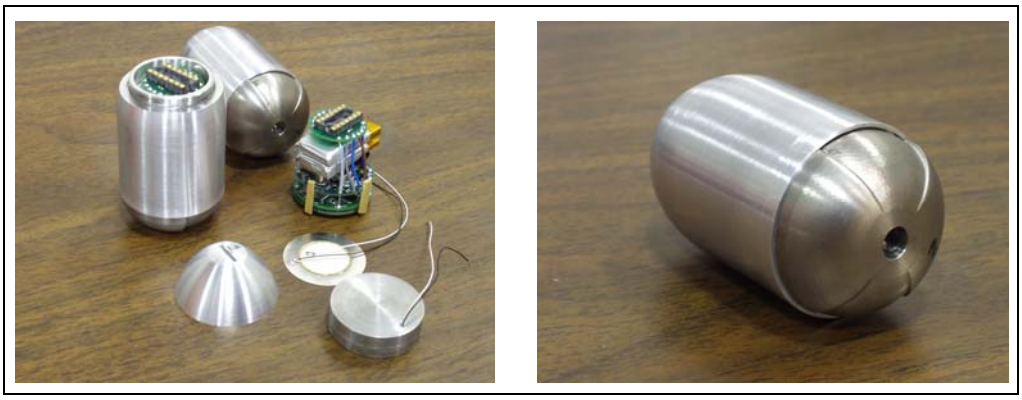

Figure 38. Photographs showing actuator disk, flight control electronics, projectile body, programming interface connector, and projectile assembly showing Coanda base configuration.

left, right, and no divert data are simulated using random initial conditions. The simulated impacts are plotted using the plus symbols. The vertical dispersion in the simulation is mostly due to muzzle velocity variation. The center of impact of the simulated vertical dispersion is indicated by a black cross. The actual open-loop test data are plotted as stars. The control authority demonstrated sufficiently eliminates all of the vertical dispersion.

3. Current and Future Program

The current program is concluding its last phase. A closed-loop test will be conducted to demonstrate that there is enough control authority to reduce the level of vertical dispersion to that of the horizontal dispersion. This is tantamount to negating the dispersion due to muzzle velocity variation. The program to date has demonstrated that MAFC can be used on subsonic projectiles and within elliptic flow fields to generate significant forces. The forces generated are capable of diverting 40-mm projectiles to levels that have tactical utility and application.

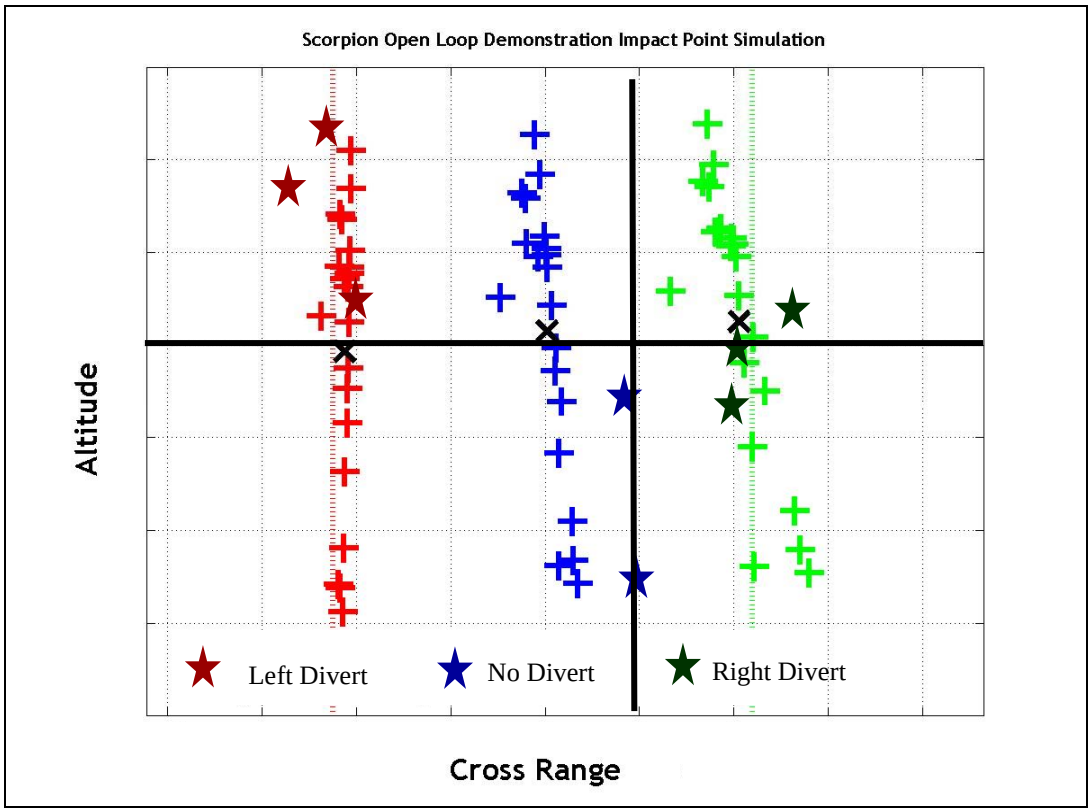

Figure 39. Comparison of simulated divert and open-loop test data.

The SCORPION program has been chosen as a DARPA demonstration program to further the application of MAFC to higher-velocity, smaller-diameter projectiles. The program will look at miniaturization of the sensor systems, higher-strength miniature combustion actuators, midbody divert schemes, effects of subsonic compressibility, higher g-load launches, and higher projectile spin rates. This level of MAFC and guided projectile technology will be required for the medium-caliber munitions being considered for the Future Combat System.

4. References

1. Rinehart, C.; McMichael, J.; Glezer, A. *Transitory Flow and Force Development on a Body of Revolution Using Synthetic Jet Actuation*; AIAA Paper No. 2003-0618, January 2003.

2. Englar, R. J. *Circulation Control Pneumatic Aerodynamics: Blown Force and Moment Augmentation and Modification; Past, Present, and Future*; AIAA Paper No. 2000-2541, June 2000.

3. Amitay, M.; Kibens, V.; Parekh, D.; Glezer, A. *The Dynamics of Flow Reattachment Over a Thick Airfoil Controlled by Synthetic Jet Actuators*; AIAA Paper No. 99-1001, January 1999.

4. Rinehart, C.; McMichael, J. M.; Glezer, A. *Synthetic Jet Based Lift Generation and Circulation Control on Axisymmetric Bodies*; AIAA Paper No. 2002-3168.

5. MetaComp Technologies. *CFD++ User Manual Version 3.5.1*; Argoura Hills, CA.

6. Sahu, J. *Unsteady Numerical Simulations of Subsonic Flow Over a Projectile With Jet Interaction*; ARL-TR-2975; U.S. Army Research Laboratory: Aberdeen Proving Ground, MD, May 2003.

7. Davis, B. S.; Brown, T. G.; Condon, D.; Hepner, D.; Myers, S. Development of an IMU/Telemetry System for Range Flight Testing of Missiles and Rockets. *Proceedings of the 18th International Ballistics Symposium*, San Antonio, TX, October 1999.

8. Harkins, T.; Davis, B. S.; Hepner, D. Novel On-Board Sensor Systems for Making Angular Measurements on Spinning Projectiles. *Proceedings of the SPIE AeroSense Symposium*, Orlando, FL, April 2001, 4365-25.

9. Hepner, D.; Hollis, M. S. L.; Mitchell, C. *Yawsonde Technology for the Jet Propulsion Laboratory Free Flying Magnetometer Program*; ARL-TR-1610; U.S. Army Research Laboratory: Aberdeen Proving Ground, MD, July 1998.

10. Newill, J. F.; Burns, B. P.; Wilkerson, S. A. *Overview of Gun Dynamics Numerical Simulations*; ARL-TR-1790; U.S. Army Research Laboratory: Aberdeen Proving Ground, MD, July 1998.

11. Whirley, R. G.; Engelmann, B. E. *DYNA3D-A Nonlinear, Explicit, Three-Dimensional Finite Element Code for Solid and Structural Mechanics*; UCRL-MA-107254, Rev. 1; Lawrence Livermore National Laboratory: Oak Ridge, TN, November 1993.

12. Huang, X.; Newill, J. F. *In-Bore Dynamic Analysis of the SCORPION Projectile*; ARL-TR-3048; U.S. Army Research Laboratory: Aberdeen Proving Ground, MD, September 2003.

13. Braun, W. F. *The Free Flight Aerodynamics Range*; BRL-R-1048; U.S. Army Ballistics Research Laboratory: Aberdeen Proving Ground, MD, July 1958.

14. Hathaway, W. H.; Whyte, R. H. *Aeroballistic Research Facility Free-Flight Data Analysis Using the Maximum Likelihood Method*; AFATL-TR-79-98; Arrow Tech Associates: South Burlington, VT, December 1979.

15. Arrow Tech Associates. *ARFDAS: Ballistic Range Data Analysis System, User and Technical Manual*; South Burlington, VT, May 1997.

16. Solid Works Corporation. *User Manual*; Vol. 1, Concord, MA, 2001.

17. Baumeister, T.; Avallone, E. *Mark's Standard Handbook for Mechanical Engineers*, 8th ed.; Kingsport Press, Inc.: New York, 1979.

18. Anderson, R. D.; Fickie, K. D. *IBHVG2 – A Users Guide*; U.S. Army Ballistics Research Laboratory: Aberdeen Proving Ground, MD, July 1987.

19. Jitpraphai, T.; Costello, M. *Dispersion Reduction of a Direct Fire Rocket Using Lateral Pulse Jets*; ARL-CR-465; U.S. Army Research Laboratory: Aberdeen Proving Ground, MD, April 2001.

NO. OF
COPIES ORGANIZATION

1 (PDF ONLY) DEFENSE TECHNICAL INFORMATION CTR
DTIC OCA
8725 JOHN J KINGMAN RD
STE 0944
FORT BELVOIR VA 22060-6218

1 US ARMY RSRCH DEV & ENGRG CMD
SYSTEMS OF SYSTEMS INTEGRATION
AMSRD SS T
6000 6TH ST STE 100
FORT BELVOIR VA 22060-5608

1 INST FOR ADVNCD TCHNLGY
THE UNIV OF TEXAS
AT AUSTIN
3925 W BRAKER LN STE 400
AUSTIN TX 78759-5316

1 DIRECTOR
US ARMY RESEARCH LAB
IMNE ALC IMS
2800 POWDER MILL RD
ADELPHI MD 20783-1197

3 DIRECTOR
US ARMY RESEARCH LAB
AMSRD ARL CI OK TL
2800 POWDER MILL RD
ADELPHI MD 20783-1197

3 DIRECTOR
US ARMY RESEARCH LAB
AMSRD ARL CS IS T
2800 POWDER MILL RD
ADELPHI MD 20783-1197

ABERDEEN PROVING GROUND

1 DIR USARL
AMSRD ARL CI OK TP (BLDG 4600)

NO. OF COPIES ORGANIZATION

3 DARPA TTO
S WALKER (2 CPS)
A MORRISH
3701 FAIRFAX DR
ARLINGTON VA 22203

1 DARPA ATO
D HONEY
3701 FAIRFAX DR
ARLINGTON VA 22203

7 GEORGIA TECH RESEARCH INSTITUTE
J MCMICHAEL (5 CPS)
K MASSEY
A LOVAS
7220 RICHARDSON RD
SMYMA GA 30080

1 OFFICE OF THE DIR OF DEFENSE
RESEARCH AND ENGRG WEAPONS
DUSD/S&T-DDR&E/WEAPONS
P MORRISON
1777 N KENT ST
` STE 9030
ROSSLYN VA 22209

1 US ARMY RESEARCH OFFICE
T L DOLIGALSKI
PO BOX 12211
RESEARCH TRIANGLE PK NC
27709-2211

1 AIR FORCE RESEARCH LAB
MUNITIONS DIR
AFRL/MNAV
G ABATE
101 W EGLIN BLVD
STE 219
EGLIN AFB FL 32542

1 OREGON STATE UNIV
DEPT OF MECHL ENGRG
M COSTELLO
CORVALLIS OR 97331

1 CDR
US ARMY ARDEC
AMSTA AR CCH
S MUSALI
PICATINNY ARSENAL NJ 07806-5000

NO. OF COPIES ORGANIZATION

2 CDR
US ARMY TANK MAIN
ARMAMENT SYSTEM
AMCPM TMA
D GUZIEWICZ
C LEVECHIA
PICATINNY ARSENAL NJ 07806-5000

1 CDR USARDEC
AMSTA AR CCH A
M PALATHINGAL
PICATINNY ARSENAL NJ 07806-5000

1 CDR US ARMY RES OFFICE
AMXRO RT IP TECH LIB
PO BOX 12211
RESEARCH TRIANGLE PK NJ
27709-2211

3 ARROW TECH ASSOC INC
R WHYTE
A HATHAWAY
H STEINHOFF
1233 SHELBOURNE RD STE D8
SOUTH BURLINGTON VT 05403

ABERDEEN PROVING GROUND

24 DIR USARL
AMSRD ARL HR SD
T MERMAGEN
AMSRD ARL WM B
J NEWILL
R COATES
AMSRD ARL WM BA
G BROWN
B DAVIS
T HARKINS
T KOGLER
D LYON
S WANSACK
M WILSON
AMSRD ARL WM BC
B GUIDOS
S SILTON
P PLOSTINS (5 CPS)
J SAHU
D WEBB
P WEINACHT
AMSRD ARL WM BF
R PEARSON
S WILKERSON

NO. OF
COPIES ORGANIZATION

AMSRD ARL WM EG
E SCHMIDT
AMSRD ARL WM TC
R SUMMERS